Automatic Selection of Optimal Savitzky-Golay Filter Parameters for Coronary Wave Intensity Analysis

Simone Rivolo[1], Eike Nagel[1], Nicolas P. Smith[2] and Jack Lee[1]

***Abstract*— Coronary Wave Intensity Analysis (cWIA) is a technique capable of separating the effects of proximal arterial haemodynamics from cardiac mechanics. The cWIA ability to establish a mechanistic link between coronary haemodynamics measurements and the underlying pathophysiology has been widely demonstrated. Moreover, the prognostic value of a cWIA-derived metric has been recently proved. However, the clinical application of cWIA has been hindered due to the strong dependence on the practitioners, mainly ascribable to the cWIA-derived indices sensitivity to the pre-processing parameters. Specifically, as recently demonstrated, the cWIA-derived metrics are strongly sensitive to the Savitzky-Golay (S-G) filter, typically used to smooth the acquired traces. This is mainly due to the inability of the S-G filter to deal with the different timescale features present in the measured waveforms. Therefore, we propose to apply an adaptive S-G algorithm that automatically selects pointwise the optimal filter parameters. The newly proposed algorithm accuracy is assessed against a cWIA gold standard, provided by a newly developed in-silico cWIA modelling framework, when physiological noise is added to the simulated traces. The adaptive S-G algorithm, when used to automatically select the polynomial degree of the S-G filter, provides satisfactory results with $\leq 10\%$ error for all the metrics through all the levels of noise tested. Therefore, the newly proposed method makes cWIA fully automatic and independent from the practitioners, opening the possibility to multi-centre trials.**

I. INTRODUCTION

Coronary Wave Intensity Analysis (cWIA) is a technique capable of separating the effects of proximal arterial dynamics from cardiac mechanics driving coronary perfusion [1]. cWIA requires simultaneous measurements of pressure and velocity waveforms at one point in a vessel and allows separation of the pressure and velocity waves travelling forward and backwards through the coronary network. Each of the 6 main waves identifiable from the cWIA output [2] are related to a specific event through the cardiac cycle (left ventricle relaxation, aortic valve closure) allowing the coronary measurements to be directly related to their physiological origin. Initially used to investigate the unique feature of the coronary blood flow of being mainly diastolic [2], [3], cWIA recently received increasing attention as a powerful technique to establish a mechanistic link between coronary haemodynamic measurements and the underlying pathopysiology [3]. More recently, De Silva et al. [4] demonstrated the prognostic value of a cWIA-derived index in predicting functional recovery following myocardial infarction.

[1]Division of Imaging Science and Biomedical Engineering, King's College London, St. Thomas' Hospital, London, United Kingdom simone.rivolo@kcl.ac.uk

[2]Faculty of Engineering, The University of Auckland, New Zealand

The clinical application of cWIA has, however, been limited by technical challenges including a lack of standardization across different studies, along with the unknown cWIA-derived indices sensitivity to the processing (Pulse Wave Speed) and pre-processing (smoothing of the acquired waveforms) parameters. Furthermore, efforts to extend cWIA to multi-centre trials have been hindered due to the strong dependency of the analysis on the specific way it is applied within individual research and clinical settings. While Siebes et al. [5] showed the low sensitivity of the cWIA outcome to error in the Pulse Wave Speed (PWS) estimation, the sensitivity of the cWIA metrics to the filtering step prior to the analysis is still unknown.

The acquired pressure and velocity signals are usually ensemble-averaged over few cardiac cycles and then smoothed using the Savitzky-Golay (S-G) filter [2]–[6] to remove the acquisition noise and estimate the signals' time derivatives, input of the cWIA. Beatwise processing has never been considered due to the strong impact that noise has on the velocity signal over a single cardiac cycle. Recently, Rivolo et al. [7] showed, using *in vivo* human and animal data, that the pressure and velocity time derivatives are strongly sensitive to the S-G parameters choice (polynomial degree N and window width M), significantly affecting, in turn, the cWIA-derived metrics (areas and peaks of the main waves). They suggested that the common practice of ensemble-averaging over few cardiac beats combined with a central finite difference scheme enhances the robustness of the cWIA. The main reason for the significant variability observed has been ascribed to the incapability of the S-G filter to deal with the different timescale features present in the velocity waveform, spanning from the relatively flat systolic plateau to the sharp early-diastolic rise.

A possible solution to overcome this limitation could be provided by a recently proposed adaptive S-G filter algorithm [6] that automatically selects pointwise the optimal S-G filter parameters (N or M). The algorithm has been developed for automatically smoothing the ECG signals and tested on simulated and real ECG data, showing promising results. Furthermore, in Rivolo et al. [7] solely the variability could be assessed since to evaluate accuracy a cWIA gold standard is required. Recently, Lee et al. [8] developed an integrative framework aimed at enabling an *in silico* cWIA. It combines the one-dimensional vascular flow modelling approach with a model of contracting myocardium that incorporates a poromechanical framework to take into account the fluid-structure interactions between the myocardium and the embedded vasculature.

The purpose of this study is, within this modelling framework, to assess the accuracy of the adaptive S-G filter with respect to the cWIA-derived metrics, when simulated physiological noise is added to the pressure and velocity waveforms. The accuracy is evaluated when ensemble-averaging is applied, imitating the clinical practise, as well as in case of beatwise processing, investigating if the adaptive S-G filter makes this novel application possible. An automatic parameter-free algorithm for cWIA pre-processing is highly desirable to eliminate the cWIA dependence on the practitioners to support potential prospective of multi-centre trials for integrating cWIA in the routine clinical practise.

II. METHODS

A brief introduction on the theoretical aspects of the cWIA theory, the adaptive S-G algorithm and the *in-silico* cWIA model is presented here. We refer to the relevant papers for an exhaustive presentation [6], [8], [9].

A. Wave Intensity Analysis

Following the in-depth overview provided by Parker [9] the main steps involved in the WIA are presented. Briefly, the beats of interest are selected and then pressure p and velocity v waveforms are ensemble-averaged in order to remove high frequency noise. The signals' time derivatives (dp, dv), input to the WIA, are computed using a 4^{th} order central finite difference scheme, since it has been shown to be optimal in reducing the outcome variability [7]. After computing the signals time derivative, the simultaneous forward and backward travelling waves can be separated, as it follows:

$$dI_{\pm} = \frac{dp_{\pm}}{dt}\frac{dv_{\pm}}{dt} = \pm\frac{1}{4\rho c}\left(\frac{dp}{dt} \pm \rho c\frac{dv}{dt}\right)^2, \qquad (1)$$

where:

$$dp\pm = \frac{1}{2}\left(dp \pm \rho c dv\right) \qquad dv\pm = \frac{1}{2}\left(dv \pm \frac{dp}{\rho c}\right). \qquad (2)$$

c represents the Pulse Wave Speed (PWS) and ρ the blood density. Dividing the time increments by dt avoids the WIA dependence to the sampling time [9]. The PWS is estimated by using the sum-of-squares method [9],

$$c = \frac{1}{\rho}\sqrt{\frac{\sum dp^2}{\sum dv^2}}, \qquad (3)$$

which is to date the only method applied in the coronary arteries [2]–[5]. It is important to note that the summations have to be taken over an integer number of cardiac periods. The cWIA-derived metrics are then defined as the main waves' integral area and peaks.

B. Adaptive Savitzky-Golay filter

The desired property of a denoising algorithm is to remove the noise introduced by the acquisition process while preserving the relevant features of the signal. Therefore, for a local polynomial regression algorithm based on the least square criterion, such as the S-G one, the question is *"Which is the optimal window width/polynomial order to be selected for the regression?"*. This problem, as shown in [6], can be solved by optimising the SURE objective (risk estimator), which is an unbiased estimator of the mean square error. Considering the smoothing process at a point n_0T, where T is the sampling time, B_{n_0} is defined as the set of samples that falls in the window width centred in n_0. The SURE risk estimator is defined as

$$\epsilon = \frac{1}{N_0}\sum_{i=1}^{N_0} f_i(\mathbf{x})^2 - \frac{2}{N_0}\sum_{i=1}^{N_0} f_i(\mathbf{x})x_i + \frac{2\sigma^2}{N_0}\sum_{i=1}^{N_0}\frac{\partial f_i(\mathbf{x})}{\partial x_i} \qquad (4)$$

where N_0 is the cardinality of the set B_{n_0}, x_i are the noisy samples and $f_i(\mathbf{x}) = \sum_{k=0}^{p} a_{k,n_0}(\mathbf{x})(nT)^k$ are the values of the fitted polynomial in the N_0 samples. The noise standard deviation σ is estimated using the median estimator [6]:

$$\sigma = \frac{\{\mathrm{median}(|x_n - x_{n-1}|; n = 2, 3, \ldots, N)\}}{0.6745}. \qquad (5)$$

A regularization term can be added to the SURE risk estimator ϵ to improve the algorithm performances in low Signal to Noise Ratio (SNR) regimes:

$$\hat{\epsilon} = \epsilon + \frac{\lambda\sigma^2}{N_0}\sum_{i=1}^{N_0}\left(\frac{\partial f_i(\mathbf{x})}{\partial x_i}\right)^2, \qquad (6)$$

where λ is a regularisation parameter that can be tuned to increase the smoothness of the filtered signal. The SURE and regularised SURE (rSURE) estimators can be used to adaptively chose the window width for a fixed polynomial degree (awS-G) or to adaptively choose the suitable polynomial degree for a fixed window width (apS-G). In both cases, for each sampling point the SURE ϵ (or rSURE $\hat{\epsilon}$) cost function is calculated for each window width value or polynomial degree and then the one providing minimum ϵ (or $\hat{\epsilon}$) is selected as optimal.

C. In silico coronary Wave Intensity Analysis

The *in silico* cWIA model, developed by Lee et al. [8], [10], allows a systematic investigation of the modulating factors underlying each wave, not achievable by means of experiments, due to physiological complexity of the system under study. It combines the one-dimensional vascular flow with a model of contracting myocardium that incorporates a poromechanical framework to describe the fluid-structure interaction between the contracting myocardium and the vessels penetrating it. The coupling between the two systems occurs both distally, at vascular termini distributed throughout the myocardium, and proximally, via the aortic sinus hemodynamics described as part of the reduced-order systemic circulation model. Rather than prescribing measured quantities as boundary conditions, the components of the model interact with one another and drive the evolution of the coronary waves. This framework thus allows the coupled wave propagation-perfusion-contraction dynamics to be studied throughout the full heart cycle. The simulations are run on a porcine cardiac geometry obtained via high-resolution cryomicrotome imaging [8], from which the myocardial mesh and a truncated vascular mesh featuring 4000 vessels were obtained. Further details of the simulation setup can be found in Lee et al. [8]. The simulated waveforms exhibits all the physiologically relevant features (Fig. 1). Moreover, the main experimentally-observed cWIA waves can be clearly identified (Fig. 1). Furthermore, the model traces are sampled at 10 kHz providing high temporal resolution test data void of noise.

D. Analysis of Adaptive S-G Accuracy

The simulated pressure and velocity waveforms are extracted in the proximal part of the LAD and the cWIA and the derived metrics are calculated and used as gold standard. The study would be focused on the integral areas, the main metric used in literature [2], [3], [5]. However, the main waves' peaks accuracy provided by the adaptive S-G algorithms is discussed in the Section IV. White Gaussian noise of 0 mean and standard deviation varying between 5 and 30, in steps of 5, is added both to a single beat and to 5 consecutive beats of the simulated velocity profile, imitating a beat-by-beat study as well as the most common practise of ensemble-averaging over few cardiac cycles. The awS-G and the apS-G algorithm, both for the SURE and rSURE estimators, are then applied on the single trace as well as pre or post ensemble-averaging over the 5 noisy beats. Based on [7], we chose a window width range where the awS-G algorithm can automatically choose the optimal M of $[7-35]$, and a polynomial range of $[1-5]$ for the apS-G algorithm. The suitable pre-selected polynomial degree and window width, for the awS-G and apS-G respectevely, are chosen based on an extensive sensitivity analysis.

Since the pressure waveform is usually of high quality in the clinical practise no noise is added. Moreover, in [7] it is shown that smoothing the ensemble-averaged pressure increases the variability of the cWIA outcome. The automatically smoothed velocity profiles are then used as an input for the cWIA analysis, outlined in Section II-A. The PWS=15 m/s derived from the simulation is used throughout the analysis. The cWIA derived metrics are then compared with the gold standard and the accuracy is assessed in terms of the percentage error defined as,

$$\text{percentage error} = \frac{(area_{i_{gold\ standard}} - area_i)}{area_{i_{gold\ standard}}} \times 100, \quad (7)$$

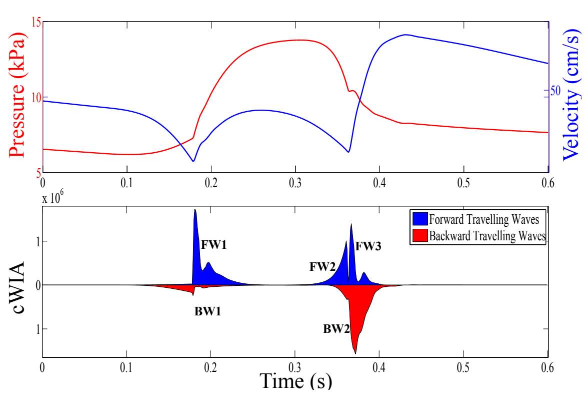

Fig. 1. The simulated traces and the resultant cWIA, both showing all the physiological main features [2], are visualised.

where the index i is referred to the cWIA waves. The percentage error is presented as mean±SD where the mean is performed over 100 experiments to avoid random noise variability. The study is performed for a sampling rate of 200 Hz and 1 kHz, typical rates used in the clinical arena.

III. RESULTS

(i) awS-G or apS-G?

The apS-G algorithm showed consistently higher accuracy amd robustness against the awS-G approach for all the metrics investigated through all the levels of noise simulated. This conclusion is valid for both the SURE and rSURE estimators for both the sampling rates investigated. Therefore, apS-G is selected for the remainder of the analysis.

(ii) apS-G sensitivity to the fixed window width

The apS-G algorithm is not strongly sensitive to the choice of the window width selected. As a matter of fact, it exhibited $\leq 10\%$ variation in the cWIA metric accuracy when the window width is varied between $[21-35]$ for 1 kHz sampling rate and between $[7-21]$ for a sampling rate of 200 Hz for both the SURE and rSURE estimators. The best performing window widths are M=27 for 1 kHz sampling rate and M=9 for 200 Hz sampling rate. These are the values used for the next steps of the analysis. The rSURE estimator for the apS-G algorithm is not strongly sensitive to the smoothing parameter λ. The sensitivity has been tested varying $\lambda = [1-10]$ in steps of 1. However, the rSURE algorithm consistently performed slightly worse ($\approx 2-3\%$) than the SURE one in terms of accuracy for all the levels of noise tested for both the sampling rates analysed. Therefore, the apS-G algorithm with the SURE risk estimator is selected for the rest of the analysis since it consistently outperformed the apS-G combined with rSURE estimator and is parameter-free.

(iii) apS-G performances

For the single trace study the apS-G algorithm using the SURE risk estimator is able to successfully ($\leq 10\%$ percentage error) remove the simulated noise for SD≤ 25 and SD≤ 20 for a sampling rate of 1 kHz and 200 Hz respectively. Considering that physiological noise is considered to be adequately simulated using SD 10, the apS-G successfully removes most of the acquisition noise.

When solely ensemble-averaging is applied acceptable accuracy ($\leq 10\%$ percentage error) is obtained only for SD$= 5$. For all the other levels of noise the percentage error is $\geq 20\%$ for all the main waves' areas for both the sampling rates investigated.

Ensemble-averaging prior to apply the apS-G algorithm consistently outperforms ($\approx 3-5\%$) the opposite procedure. Ensemble-averaging and than applying apS-G algorithm with SURE risk estimator provides satisfactory results, successfully providing a percentage error of $\leq 10\%$ through all the metrics, for all the levels of noise and for both the sampling rates analysed (Table I). The most sensitive metric to the noise is the area of FW3. This is mainly due to the relative

TABLE I

THE PERCENTAGE ERROR IS LISTED FOR THE APS-G SMOOTHING POST-ENSEMBLE-AVERAGING FOR 200 HZ AND 1 KHZ SAMPLING RATE.

	Ensemble-Averaging→apS-G 200 Hz						Ensemble-Averaging→apS-G 1 kHz					
Noise	SD 5	SD 10	SD 15	SD 20	SD 25	SD 30	SD 5	SD 10	SD 15	SD 20	SD 25	SD 30
FW1	1.4±0.8	2±1.7	3.3±2.2	4±2.4	4.7±3	4.4±3.4	3.2±0.6	2.7±1.2	1.9±1.5	2±1.7	3.2±2.1	4.3±2.8
FW2	3.2±1.6	3.9±2.9	5±3.8	6.1±4	7.8±6.1	9±6.4	3.6±1	3.5±1.7	3.3±2.2	3.1±2.3	3.6±2.8	5.1±3.5
FW3	1.4±1	2.8±2.2	4.7±3.9	5.2±3.9	8±6.1	9.6±7	10.4±1.6	9.9±2.1	8.7±3.1	7.7±3.9	6.7±4.5	6.2±4.7
BW1	1.44±0.8	2±1.7	3.3±2.2	4±2.4	4.7±3	4.4±3.3	3.2±0.6	2.7±1.2	1.9±1.5	2.1±1.7	3.2±2.1	4.2±2.8
BW2	2±1.2	3±2.2	4.3±3.4	4.9±3.7	7.1±5.6	8.9±6.3	7.1±0.9	6.7±1.7	5.9±2.6	5.2±3.06	4.4±3.3	5±3.6

short duration and the proximity to FW2. If FW3 is excluded from the analysis, the percentage error is $\leq 5\%$ for all the remaining metrics for most of the levels of noise tested.

(iv) PWS estimation

The simulated PWS=15 m/s has been used for the cWIA in order to assess the adaptive S-G filter performances independently to an error in the PWS estimation. However, it is crucial to assess how the sum-of-squares method performs in case of de-noised traces, since the exact PWS is unknown in the clinical practise. Applying the sum-of-squares method to the simulated traces provides PWS$=12.97$ m/s. When the sum-of-squares method is applied to the denoised traces the maximum estimation error obtained is $\approx 30\%$ for the single trace case, which is significantly below the $\pm50\%$ estimation error threshold range in which the cWIA is insensitive to a PWS variation [5]. Moreover, if ensemble-averaging is applied, for both 200 Hz and 1 kHz, the PWS estimation error drops below 10% (Figure 2). It is therefore recommended to apply the sum-of-squares method over the ensemble-averaged traces for the PWS estimation, and then use it for both the multi trace or beat-by-beat study.

IV. DISCUSSION AND CONCLUSION

We implemented and tested an adaptive S-G algorithm to automatically smooth the acquired pressure and velocity waveforms making, for the first time, cWIA a fully automated analysis. The percentage error in the cWIA derived metrics obtained applying the apS-G algorithm post ensemble-averaging, combined with the SURE risk estimator, is $\leq 10\%$ for all the metrics through all the levels of noise tested (Table I). Moreover, the error in the estimated PWS

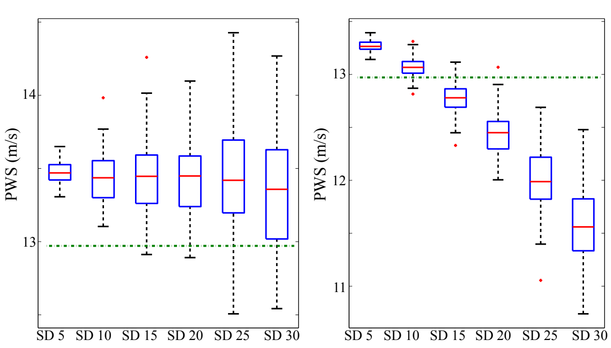

Fig. 2. The estimated PWS by means of sum-of-squares method applied to the ensemble-averaged and apS-G denoised traces is compared to the gold standard one (green dashed line) for both sampling rates analyzed.

is within the range where the cWIA has been demonstrated not to be sensitive [5]. Furthermore, we have shown that the strategy suggested in [7] of relying solely on the ensemble-averaging over few beats is valid only for low levels of noise (SD$=5$). If beatwise study are of interest apS-G provides a high level of accuracy for physiological range of noise, up to SD≤ 25, above which the percentage errors rises to $\approx 15\%$. When the peaks of the main waves are of interest, the percentage error rises to a range of $\approx 15-20\%$ for both the sampling rates analysed. The lower accuracy in the waves' peaks is not surprising since they are the results of a product of two time derivatives resulting in a strong amplification of the acquisition noise.

In conclusion, as a guideline for the clinicians applying cWIA, the apS-G algorithm combined with the SURE risk estimator (with M=9 for 200 Hz and M=27 for 1 kHz) provides an accurate and fully automatic method to obtain the cWIA-derived metrics from acquired waveforms, therefore eliminating the cWIA dependency on the practitioners.

ACKNOWLEDGMENT

This study was supported by the British Heart Foundation Centre of Research Excellence hosted at King's College under grant number BHF RE/08/003. The authors acknowledge financial support from the Department of Health via the National Institute for Health Research (NIHR) comprehensive Biomedical Research Centre award to Guy's & St Thomas' NHS Foundation Trust in partnership with King's College London and King's College Hospital NHS Foundation Trust.

REFERENCES

[1] A. D. Hughes et al., "Waves in arteries: A review of wave intensity analysis in the systemic and coronary circulations," *Art. Res.*, vol. 2, no. 2, pp. 51–59, May 2008.

[2] J. E. Davies et al., "Evidence of a dominant backward-propagating "suction" wave responsible for diastolic coronary filling in humans, attenuated in left ventricular hypertrophy." *Circ.*, vol. 113, no. 14, pp. 1768–78, Apr. 2006.

[3] A. Kyriacou et al., "Improvement in Coronary Blood Flow Velocity with Acute Biventricular Pacing is Predominantly Due to an Increase in a Diastolic Backward-Travelling Decompression (Suction) Wave." *Circ.*, Aug. 2012.

[4] K. De Silva et al., "Coronary Wave Energy: A Novel Predictor of Functional Recovery After Myocardial Infarction." *Circ.*, Mar. 2013.

[5] M. Siebes et al., "Potential and limitations of wave intensity analysis in coronary arteries." *MBEC*, vol. 47, no. 2, pp. 233–9, Feb. 2009.

[6] S. R. Krishnan et al., "On the Selection of Optimum Savitzky-Golay Filters," *IEEE Trans. on Signal Proc.*, vol. 61, pp. 380–391, 2013.

[7] S. Rivolo et al., "Enhancing Coronary Wave Intensity Analysis Robustness by High Order Central Finite Differences," *Art. Res.*, 2014.

[8] J. Lee et al., "In-silico coronary wave intensity analysis," *submitted to JP*, 2014.

[9] K. H. Parker, "An introduction to wave intensity analysis," *MBEC*, vol. 47, no. 2, pp. 175–188, 2009.

[10] J. Lee et al., *Multiscale Modelling of Cardiac Perfusion*. Submitted for inclusion in The Cardio-circulatory System: from Modelling to Clinical Applications. A. Quarteroni, 2014.